JOURNAL OF ENGINEERING SCIENCES

Volume 8, Issue 2 (2021)

Chelabi M. A., Basova Y., Hamidou M. K., Dobrotvorskiy S. (2021). Analysis of the three-dimensional accelerating flow in a mixed turbine rotor. Journal of Engineering Sciences, Vol. 8(2), pp. D1-D7, doi: 10.21272/jes.2021.8(2).d1

Analysis of the Three-Dimensional Accelerating Flow in A Mixed Turbine Rotor

Chelabi M. A.[1*[0000-0002-4880-9496]], Basova Y.[2[0000-0002-8549-4788]], Hamidou M. K.[1], Dobrotvorskiy S.[2[0000-0003-1223-1036]]

[1] Laboratory of Applied Mechanics, Faculty of Mechanical Engineering, University of Science and Technology Mohamed Boudiaf-El Mnouar, PO Box 1505 Bir El Djir 31000 Oran, Algeria;
[2] Department of Mechanical Engineering Technology and Metal-Cutting Machines, Educational and Scientific Institute of Mechanical Engineering and Transport, National Technical University "Kharkiv Polytechnic Institute", 2, Kyrpychova St., 61002 Kharkiv, Ukraine

Article info:
Submitted: July 19, 2021
Accepted for publication: November 17, 2021
Available online: November 22, 2021

***Corresponding email:**
chelabilma.usto@yahoo.com

Abstract. An investigation on new rotor blade designs conceived to produce higher exit relative kinetic energy of a mixed flow turbine is undertaken. Accelerating the flow through the rotor in a relative frame of reference improves energy transfer to the shaft, which is only produced in a rotating rotor. A three-dimensional converging rotor channel might respond to the analysis requirements in the subsonic flow regimes. Effectively, the machine experiences a 3.71 % and 3.67 % increase in work output and efficiency, respectively, representing this study's primary intent. This has been accomplished by varying the shroud profile to a lesser eye tip diameter, then the hub profile to a larger eye root diameter. At last, both shroud and hub profiles are varied. It appears possible to enhance the performance of the rotor in terms of optimum work done and efficiency by devising suitable blade geometry designs. ANSYS CFX 15 is the code of all simulation works.

Keywords: blade, vane-to-vane plane, hub, shroud, meridional plane.

1 Introduction

The mixed inflow turbines combine the advantages of both the axial and the radial types. They can use higher flow rates and operate at a higher specific rate. The maximum efficiency is attained at a lower ratio of tip speed over the velocity. The bending stresses on the new blade geometry are lesser compared to the radial turbines. Also, the use of variable nozzle blades is efficient even at off-design point operation. This type of turbine covers large ranges of power, rate of mass flow, and rotational speeds. Among their applications, one cites Diesel engines in pulsating flow regimes.

One is concerned with the rotor through-flow area effect on the turbine performance. It must be observed that the rotor channel cross-sectional area, from inlet to exit, is designed to ensure specific variations during the gas expansion. Besides, it is pointed out that on the one hand, the passe of the flow in the vane-to-vane Plane is converging, which implies flow acceleration in the moving reference frame for subsonic flow regimes. On the other hand, the meridional channel surface is diverging. The main reason for this design is to increase the specific volume during the fluid flow expansion, which would require an increase in flow area. Since the flow regime is subsonic, a flow deceleration is expected. Apparently, the flow parameters are affected by the combined effects of the sidewalls of the rotor channel. As a result, a little change in the relative velocity is revealed. Based on these arguments, investigations regarding the blade geometry are undertaken to shape a three-dimensional converging rotor through a flow sectional area for achieving greater flow acceleration rates. This might cause energy transformation into relative kinetic energy with greater energy transfer to the rotor into higher specific output work done.

A few arrangements might be employed to design new blade configurations for the analysis. A numerical simulation using Ansys ICEM is adopted to explore the feasibility and the physical significance of the proposed design cases. The quantities and the geometry of the mixed inflow turbine rotor relative to which the results of the present study may be compared are those of the turbine designed and tested at Imperial College of London. Several research works have been conducted on this mixed turbine. One might cite papers related to the team of the Laboratory of Applied Mechanics of Oran-Algeria.

2 Literature Review

Abidat et al. [1] designed and analyzed the volute of a radial and a mixed flow turbine, Litim et al. [2] studied the effect of blade number on the mixed inflow turbine performances. Maghnine et al. [3] presented the influence of volute cross-section shape on the mixed inflow turbine performances. Hamel et al [4] investigated a twin entry flow turbine volute. In papers [5-7] presented the aerodynamic performance of the mixed flow turbine blade design. Bencherif et al. [8] studied the unsteady performance of a twin-entry mixed flow turbine. Abidat [9] and Abidat et al. [10] developed a new method of blade profile generation using the Bezier polynomials. The works [11-12] include research to ensure high-quality mechanical machining of turbine blades for regular operation. Abidat et al. [13] studied the clearance effect between the rotor blades and the casing on the mixed turbine performance. In two cases, papers [14, 15] studied the effects of the cone and the inlet blade angles on mixed inflow turbine performance. The first is for a fixed outlet volute section and the second for a variable outlet volute section. Some geometric parameters were held fixed to keep the same rotor casing. Other researchers have examined this type of turbine; Rajoo et al. [16] offered a comprehensive review of mixed-flow turbines. Palfreyman et al. [17] obtained the rotor geometry of the mixed flow turbine by radially scanning the leading edge of a radial turbine. Whitfield et al. [18] established a relationship between the blade angle, the cone angle, and the camber angle. Watson et al. [19] compared the efficiency of axial, radial, and mixed turbines for different speed ratios and worked to improve the performance of the turbocharged engine with variable geometry. Pesiridis [20], Pesiridis and Martinez-Botas [21–23] modified the mechanism of actuation of sliding vanes to adapt to the nature of pulsating flow of the exhaust gas by inducing artificially sinusoidal motion. Wallace and Blair [24] reported the earliest experimental study of the irregular flow effect on mixed inflow turbine performance. Yamaguchi et al. [25] analyzed four rotors of mixed inflow turbines having different camber curves. Ketata et al. [26] studied a Mixed Flow Turbine Volute numerically Operating in Various Steady Flow Conditions. Leonard et al. [27] studied the inlet mixed inflow turbine geometry. Bernhardt Lüddecke et al. [28] compared the efficiencies of mixed and radial inflow turbines for different rotational speeds. Padzillah et al. [29] studied numerically and experimentally the flow angle effect on mixed inflow turbine performance and discovered that only one rotor blade part operates in optimal conditions.

3 Research Methodology

3.1 Initial rotor design

The rotor of the mixed inflow turbine under examination is a constant blade angle type, named type A. Since the meridian plane of the rotor represents maim interest of this study, it is profitable to have its description given in Figure 1. The values of the geometrical parameters are represented in Table 1. As stated before, changes will be made to the shroud and the hub profiles. For all the subsequent calculations, the optimum expansion ratio is adopted, which is equal to 2.91. It is retained from ABIDAT's thesis analysis [30].

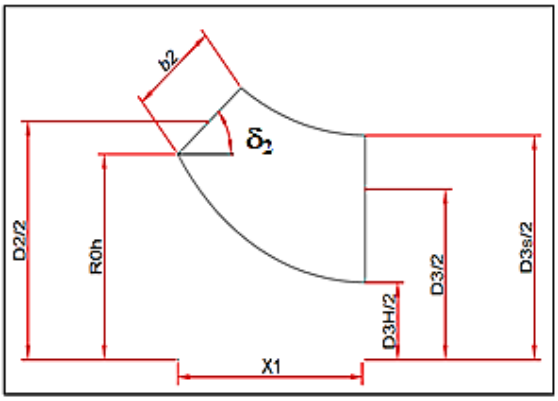

Figure 1 – The blade meridian view

Table 1 – The geometrical parameter values (mm)

b_2	D_2	R_{0h}	X_1	D_{3H}	D_3	D_{3S}	δ_2(°)
17.99	83.58	36	40	27.07	59.7	78.65	40

3.2 A new design approach

The new rotor impellers under consideration are designed as follows. To lessen the degree of the meridional plane surface divergence, the first alternative is achieved by lowering the blade's eye tip diameter, which implies lowering the shroud profile as shown in Figure 2.

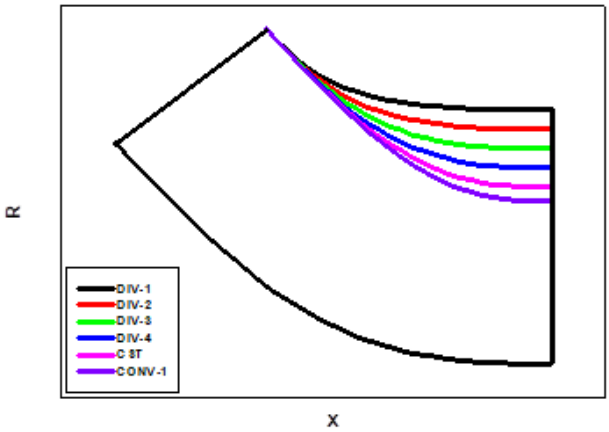

Figure 2 – Different blade meridian views
for different shroud exit diameters

The second alternative would be lifting the hub profile for a higher eye root diameter as depicted in Figure 3. Finally, both shroud and hub profiles vary for a smaller exit diameter, as presented in Figure 4. The initial rotor design taken as a reference for comparison will be called: Div-1.

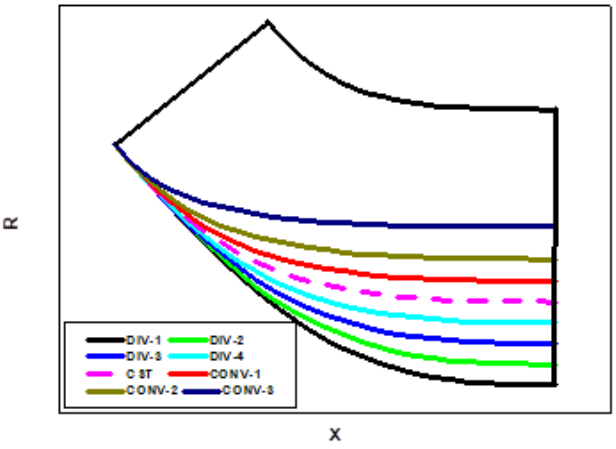

Figure 3 – Different blade meridian views for different hub exit diameters

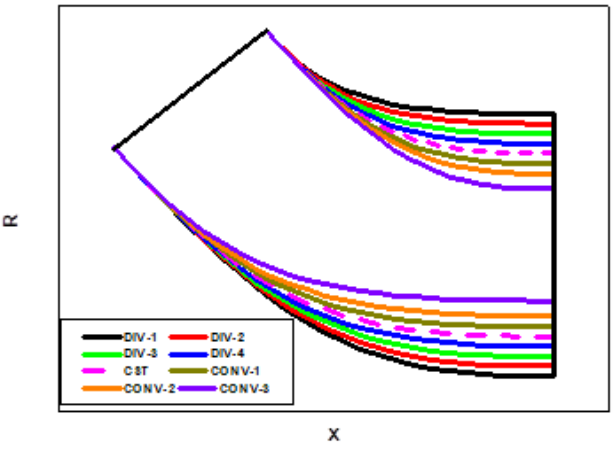

Figure 4 – Different blades meridian view by changing of hub and shroud diameters

3.3 Rotor blade profile generation

The method for designing the blade profile of the mixed turbine rotor is to use the pressure balance flow path principle by considering the faces acting on a particle fluid flow in a rotor path. The Bezier polynomial is adopted for the shape generation of the rotor under examination. The following expression gives the radius:

$$r = (1-u)^4 r_0 + 4u(1-u)^3 r_1 + 6u^2(1-u)^2 r_c + \\ +4u^3(1-u)r_2 + u^4 r_3. \quad (1)$$

The distance in the axial direction is presented by the following equation:

$$x = (1-u)^4 x_0 + 4u(1-u)^3 x_1 + 6u^2(1-u)^2 x_c + \\ 4u^3(1-u)x_2 + u^4 x_3. \quad (2)$$

The leading edge is obtained by the following relations:

$$\theta = \theta_{ref} + \frac{1}{\sin(\delta_2)} \int_{x_{ref}}^{x} \tan(\beta_{2b}) \frac{dx}{r}, \quad (3)$$

$$r = r_{0h} + (x - x_{0h}) \tan(\delta_2). \quad (4)$$

The following equations calculate the trailing edge:

$$\boldsymbol{x = (1-u)^4 x_0 + 4u(1-u)^3 x_1 + 6u^2(1-u)^2 x_b + \\ +4u^3(1-u)x_2 + u^4 x_3,} \quad (5)$$

$$\boldsymbol{\theta = (1-u)^4 \theta_0 + 4u(1-u)^3 \theta_1 + 6u^2(1-u)^2 \theta_b + \\ + 4u^3(1-u)\theta_2 + u^4 \theta_3.} \quad (6)$$

The camberline blade is shown in Figure 5.

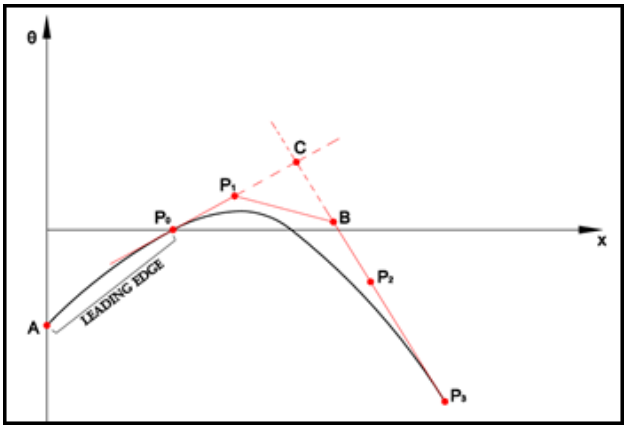

Figure 5 – The camberline blade view

The three-dimensional blade profiles are depicted in Figure 6 corresponding to the case hub held fixed; Figure 7 corresponds to the casing shroud held fixed and the last on Figure 8 corresponds to the case where both hub and shroud are varied. Each meridional plane surface is defined by the ratio of the cross-sectional area, exit over inlet sections. Depending on them through flow sectional area shape; they are called DIV for diverging, CST for constant, and CONV for converging channels.

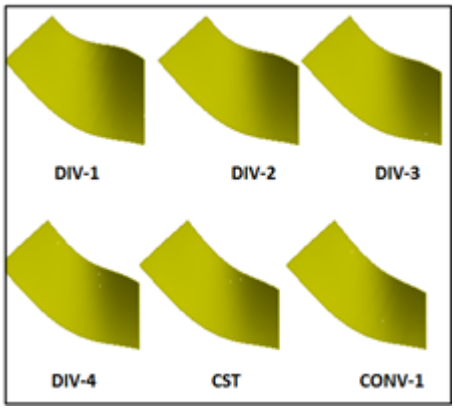

Figure 6 – Blade geometrical shape views for different shroud exit diameter

3.4 Mesh optimization and Numerical model validations

The unstructured hexahedral grid is used because it responds well with turbomachine simulations.

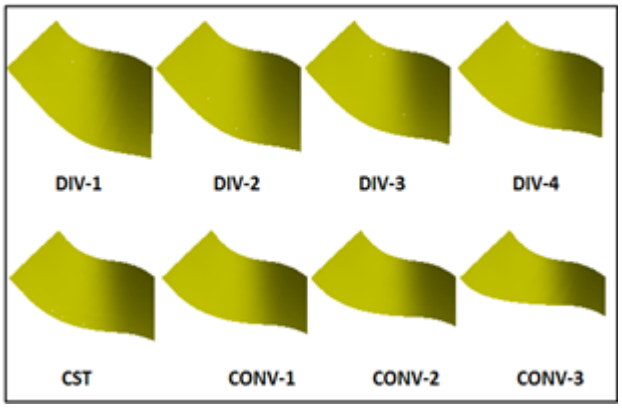

Figure 7 – Blade geometrical shape views for different hub exit diameter

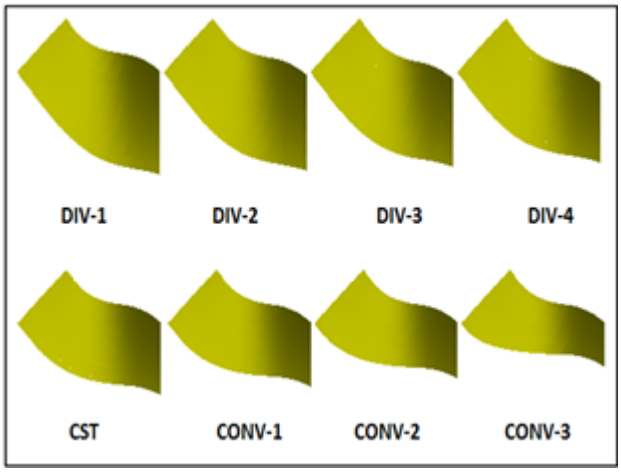

Figure 8 – Blade geometrical shape views for different hub and shroud exit diameters

Because the numerical simulation solutions are only approximations, the analysis of mesh quality and its influence on the results deserve particular attention. The numbers of mesh elements tested are 107 214, 233 814, 333 372, and 415 030. The analysis of the graphs shows that the number of elements does not have any influence on the torque and the mass flow rate (Figure 9), a negligible influence on the static pressure distribution around the rotor blade (Figure 10). On the other hand, there exists a variation in the efficiency graph. Figure 9 shows that the optimal grid number is higher or equal to 333372 elements which are applied in the numerical simulations.

The numerical validation is confirmed by the experimental works of Chen and Abidat [10] on rotor type A. The pressure ratio is defined as the total pressure at the inlet relative to the static pressure at the outlet; the distribution is in the axial direction of the blade. The results are shown in Figure 11. A good agreement between numerical simulations and experimental results is remarked.

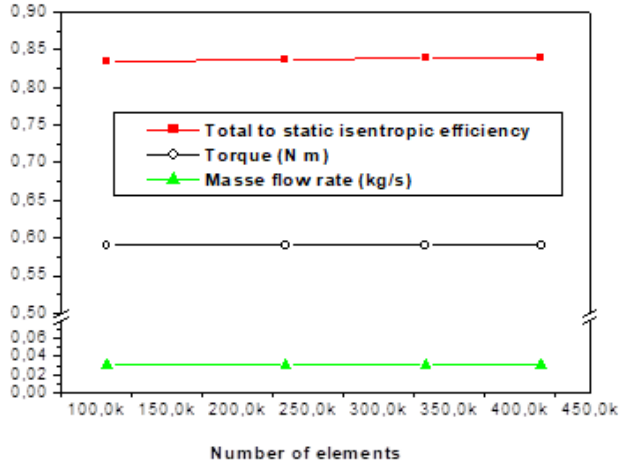

Figure 9 – Effect of element number on efficiency, torque and mass flow rate

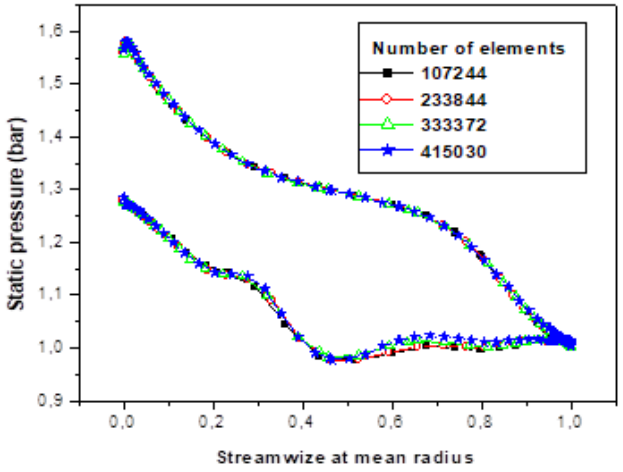

Figure 10 – Effect of element number on static pressure

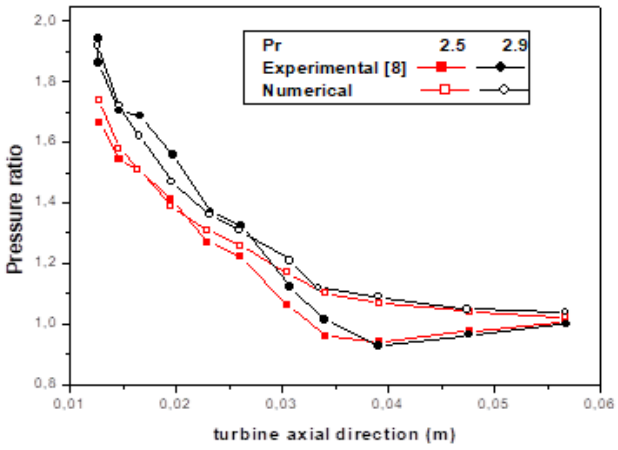

Figure 11 – Numerical result validation

4 Results and Discussion

The channel geometry of the rotor has a significant influence on the flow, on the energy transformation of the turbine. For the sake of comparison, the simulation results for the three alternatives at full rotational speed are

reported on the same diagram versus cases of channel geometries. The first alternative, which corresponds to the analysis of a blade shroud varied in profile shape keeping the hub profile unchanged, reveals relatively poor performance variables. The optimum design case remains for a diverging meridional plane surface, namely the Div-3 case for a maximum output work (Figure 12) and the Div-2 case for a maximum power developed (Figure 13).

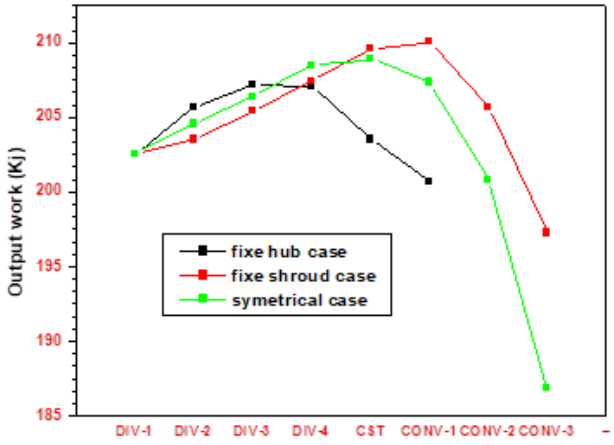

Figure 12 – Output work at 98 000 rpm for three alternatives

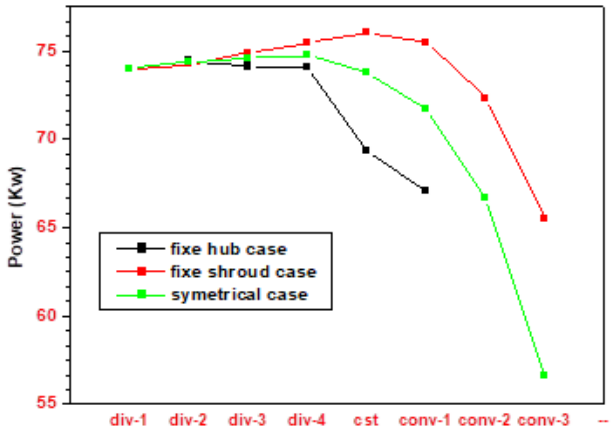

Figure 13 – Power at 98 000 rpm for three alternatives

Then, the channel convergence effect ceases to have significance in terms of beneficial gains.

This is observed by a faster fall off the mass flow rate (Figure 14), the output work (Figure 12), the power developed (Figure 13), and the efficiency (Figure 15). When keeping the shroud profile fixed and varying the hub profile, which represents the second alternative, the most efficient rotor blade profile for the best effect on the work generation is obtained. The Conv-1 case is retained for its maximum output work, but the Const case for its maximum power developed. This is probably due to the fluid deflection and compression effects by the new curvature of the meridional streamline and the vane-to-vane plane curvature. A remarkable feature is noticed, although the flow passage is restricted from a design case to the next one for a smaller exit area, the mass flow rate remains almost invariable from the initial design case: Div-1 until the Conv-1 design case. Then it falls off as depicted in Figure 14.

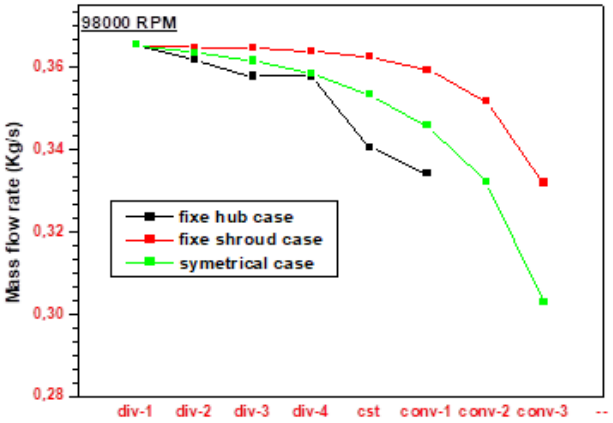

Figure 14 – Power at 98 000 rpm for three alternatives

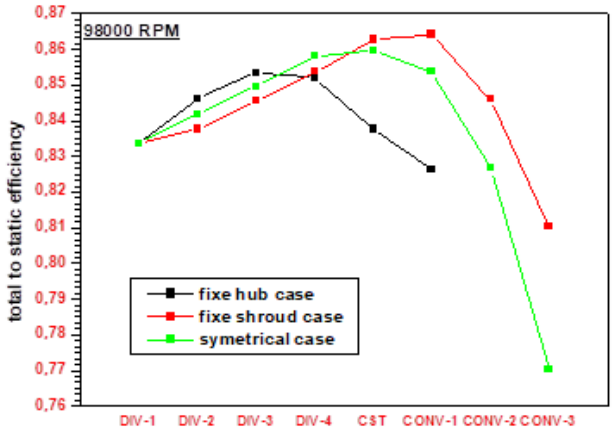

Figure 15 – Total to static efficiency for three alternatives

All the performance parameters are more significant than the two other alternatives seen in Figures 12–15. The channel aerodynamic shape is adequate for transforming the inlet available energy into shaft work. The last alternative where both hub profile and shroud profile are varied, named the symmetric case, approaches the performances of the second alternative. The Const design case shows maximum output work and the Div-4 design case for maximum power output, as reported in Figures 12–13. Based on the simulation results, the estimated gains (% increase) compared to the initial design case: Div-1, for the three alternatives, are listed in Table 2.

The decisive advantage of either a maximum power developed or a maximum efficiency (max output work) represents a compromise between two different aerodynamic blade profiles.

Table 2 – Maximum gain estimation for three alternatives

Case	Maximum gain	Geometry	Mass flow rate, %	Output work, %	Power, %	Total to static efficiency, %
Fixe hub	Power	DIV-2	–0.93	1.54	0.59	1.52
	Output work	DIV-3	–2.06	2.29	0.18	2.27
Fixe shroud	Power	CST	–0.72	3.49	2.74	3.49
	Output work	CONV-1	–1.63	3.71	2.02	3.67
Symmetrical	Power	DIV-4	–1.89	2.93	0.99	2.94
	Output work	CST	–3.27	3.13	–0.24	3.13

5 Conclusions

Several channel geometry configurations have been explored to increase the energy transformation. The interdependence of the flow parameters and the complex three-dimensionality of the machine reveals some instructive results. Effectively, the analysis based on channel argument appears suitable for specific rotor designs, which confirm improvement in the turbine performance.

Their effects on the work generation capacity are observed. We retain from the analysis. It appears that for each alternative, two facets emerge. The maximum obtained in the output work is related to the maximum efficiency for a specific optimum design case. But the maximum power developed are recorded the maximum expansion ratio and the minimum absolute kinetic energy at the rotor exit, corresponding to a different geometrical design optimum case. The same rule is noticeable for the three considered alternatives. It arises from the wall channel combinations a remarkable feature that a three-dimensional converging rotor cross-sectional area is not a necessary and sufficient condition to increase the relative kinetic energy.

Nomenclature

D_2	Mean diameter at rotor inlet
b_2	Blade height at rotor inlet
δ_2	Cone angle at rotor inlet
D_3	Exducer hub diameter
D_{3S}	Exducer tip diameter
$X1$	Length of the rotor
θ	Camber angle
θ_{ref}	Reference camber angle
x_{ref}	Reference axial distance of the blade
β_{2b}	Mean blade angle at rotor inlet
R_{0h}	The radius at the tip rotor inlet.
x_{0h}	The axial distance for the initial point of the hub.
D_3	Exducer root mean square diameter
X	Axial polar variable
r	Radial polar variable
u	variable between 0 and 1

References

1. Hamel, M., Hamidou, M. K., Cherif, H. T., Abidat, M., Litim, S. A. (2008). Design and flow analysis of radial and mixed flow turbine volutes. *ASME Turbo Expo*. ASME, New York. Vol. 1(PART C), pp. 2329-2333, doi: 10.1115/GT2008-50503.
2. Ali, L. S., Mohammed, H., Kamel, H. M. (2017). The number of blade effects on the performance of a mixed turbine rotor. *Engineering Review*, Vol. 37(3), pp. 349-360.
3. Meghnine, M. A., Hamidou, M. K., Hamel, M. (2017). Influence of the volute cross-sectional shape on mixed inflow turbine performances. *Advances in Mechanical Engineering*, Vol. 9(7), pp. 1-15, doi: 10.1177/1687814017708174.
4. Hamel, M., Bencherif, M. M., Hamidou, M. K. (2017). Investigation of a twin entry mixed flow turbine volute, benefits with regard to the eco-system. *Materials Physics and Mechanics*, Vol. 32(1), pp. 31-42.
5. Omar, Z. K., Mohammed, H., Kamel, H. M. (2017). Computational aerodynamic performance of mixed-flow turbine blade design. *Engineering Review*, Vol. 37(2), pp. 201-213.
6. Leonard, T., Spence, S., Filsinger, D., Starke, A. (2020). Design and performance analysis of mixed flow turbine rotors with extended blade chord. *Journal of Turbomachinery*, Vol. 142(12), 121003. doi: 10.1115/1.4047894.
7. Lee, S. P., Barrans, S. M., Nickson, A. K. (2021). The impact of volute aspect ratio and tilt on the performance of a mixed flow turbine. *Proceedings of the Institution of Mechanical Engineers, Part A: Journal of Power and Energy*, Vol. 235(6), pp. 1435-1450, doi: 10.1177/0957650921998228.
8. Bencherif, M. M., Hamidou, M. K., Hamel, M., Abidat, M. (2016). Study of unsteady performance of a twin-entry mixed flow turbine. *Journal of Applied Mechanics and Technical Physics*, Vol. 57(2), pp. 300-307, doi: 10.1134/S0021894416020139.
9. Rajeevalochanam, P., Sunkara, S. N. A., Mayandi, B., Banda, B. V. G., Chappati, V. S. K., Kumar, K. (2016). Design of highly loaded turbine stage for small gas turbine engine. *ASME Turbo Expo 2016: Turbomachinery Technical Conference and Exposition, GT 2016*. Seoul, South Korea, Vol. 2C-2016, 123972, doi: 10.1115/GT2016-56178.

10. Chen, H., Abidat, M., Baines, N. C., Firth, M. R. (1992). The effects of blade loading in radial and mixed flow turbines. *ASME 1992 International Gas Turbine and Aeroengine Congress and Exposition, GT 1992*, Cologne, Germany, Vol. 1, 111210, doi: 10.1115/92-GT-092.
11. Kononenko, S., Dobrotvorskiy, S., Basova, Y., Gasanov, M., Dobrovolska, L. (2019) Deflections and frequency analysis in the milling of thin-walled parts with variable low stiffness. *Acta Polytechnica*, Vol. 59(3), pp. 283-291, doi: 10.14311/AP.2019.59.0283.
12. Dobrotvorskiy, S., Kononenko, S., Basova, Y., Dobrovolska, L., Edl, M. (2021). Development of optimum thin-walled parts milling parameters calculation technique. *4th International Conference on Design, Simulation, Manufacturing: The Innovation Exchange, DSMIE 2021*, Lviv, Ukraine, Vol.2021, pp. 343-352, doi: 10.1007/978-3-030-77719-7_34.
13. Abidat, M., Hamidou, M. K., Hachemi, M., Hamel, M., Litim, S. A. (2008). Performance prediction of a mixed flow turbine. *Mecanique et Industries*, Vol. 9(1), pp. 71-79, doi: 10.1051/meca:2008009.
14. Chelabi, M. A., Hamidou, M. K., Hamel, M. (2017). Effects of cone angle and inlet blade angle on mixed inflow turbine performances. *Periodica Polytechnica Mechanical Engineering*, Vol. 61(3), pp. 225-233, doi: 10.3311/PPme.9890.
15. Lee, S. P., Jupp, M. L., Barrans, S. M., Nickson, A. K. (2019). Analysis of leading edge flow characteristics in a mixed flow turbine under pulsating flows. *Proceedings of the Institution of Mechanical Engineers, Part A: Journal of Power and Energy*, Vol. 233(1), pp. 78-95, doi: 10.1177/0957650918778661.
16. Rajoo, S., Martinez-Botas, R. (2008). Mixed flow turbine research: A review. *Journal of Turbomachinery*, Vol. 130(4), 044001, doi: 10.1115/1.2812326.
17. Palfreyman, D., Martinez-Botas, R.F. (2002). Numerical study of the internal flow field characteristics in mixed flow turbines. *American Society of Mechanical Engineers, International Gas Turbine Institute, Turbo Expo (Publication) IGTI*, Vol. 5(A), pp. 455-472, doi: 10.1115/GT2002-30372.
18. Whitfield, A., Baines., N.C. (1990). *Design of radial turbomachines* (1st ed.). Harlow, Essex, England: Longman Scientific and Technical, Wiley, New York, USA.
19. Watson, N., Janota, M. S. (1982). *Turbocharging the Internal Combustion Engine* (1st ed.). Palgrave, Kent. doi: 10.1007/978-1-349-04024-7.
20. Pesiridis, A. (2007). *Turbocharger Turbine Unsteady Aerodynamics with Active Control*. PhD Thesis, Imperial College, London, UK.
21. Pesiridis, A., Martinez-Botas, R. F. (2007). Experimental evaluation of active flow control mixed-flow turbine for automotive turbocharger application. *Journal of Turbomachinery*, Vol. 129(1), pp. 44-52, doi: 10.1115/1.2372778.
22. Pesiridis, A., Martinez-Botas, R. F. (2006). Active control turbocharger for automotive application: An experimental evaluation. *Conference: 8th International Conference on Turbocharging and Turbochargers*, CRC Press, London, pp. 223-232, doi: 10.1016/B978-1-84569-174-5.50020-8.
23. Pesiridis, A., Martinez-Botas, R. F. (2005). Experimental evaluation of active flow control mixed-flow turbine for automotive turbocharger application. *ASME Turbo Expo 2005 - Gas Turbie Technology: Focus for the Future*, Reno-Tahoe, Nevada, USA, Vol. 6(B), GT2005-68830, pp. 881-895, doi: 10.1115/GT2005-68830.
24. Wallace, F. J., Blair, G. P. (1965). The pulsating-flow performance of inward radial-flow turbines. *ASME 1965 Gas Turbine Conference and Products Show*, Vol. 1-A, 113390, doi: 10.1115/65-GTP-21.
25. Yamaguchi, H., Nishiyama, T., Horiai, K., Kasuya, T. (1984). High performance Komatsu KTR150 turbocharger. *SAE*, 840019, doi: 10.4271/840019.
26. Ketata, A., Driss, Z. (2017). Numerical study of a vanned mixed flow turbine operating in various steady flow conditions. *International Journal of Mechanics and Applications*, Vol.7(1), pp. 24-30, doi: 10.5923/j.mechanics.20170701.03.
27. Leonard, T., Spence, S., Early, J., Filsinger, D. (2013). Numerical study of a vanned mixed flow turbine operating in various steady flow conditions. *6th International Conference on Pumps and Fans with Compressors and Wind Turbines, ICPF 2013*, Beijing, China, 52(TOPIC 4), 042012, doi: 10.1088/1757-899X/52/4/042012.
28. Luddecke, B., Filsinger, D., Ehrhard, J. (2012). On mixed flow turbines for automotive turbocharger applications. *International Journal of Rotating Machinery*, Vol. 2012, 589720, doi: 10.1155/2012/589720.
29. Padzillah, M. H., Rajoo, S., Martinez-Botas, R. F. (2015). Experimental and numerical investigation on flow angle characteristics of an automotive mixed flow turbocharger turbine. *Jurnal Teknologi*, Vol. 77(8), pp. 7-12, doi: 10.11113/jt.v77.6148.
30. Abidat, M., Chen, H., Baines, N. C., Firth, M. R. (1992). Design of a highly loaded mixed flow turbine. *Proceedings of the Institution of Mechanical Engineers, Part A: Journal of Power and Energy*, Vol. 206(2), pp. 95-107, doi: 10.1243/PIME_PROC_1992_206_016_02.